Progress In Electromagnetics Research M, Vol. 59, 55–64, 2017

Electromagnetic Scattering from 1-D Sea Surface with Large Windspeed by Using Iterative Physical Optics Algorithm

Juan Li*, Ke Li, and Li-Xin Guo

Abstract—In the paper, the electromagnetic scattering (EM) from a one-dimensional (1-D) perfectly electric conducting (PEC) randomly rough sea surface with large windspeed is investigated by the iterative physical optics (IPO) algorithm. In this method the multiple coupling interactions among points on sea surface are considered. To improve computational efficiency, the local coupling technique is adopted to accelerate the iterative process. In numerical results, the EM scattering by 1-D sea surface for different polarizations is calculated and compared with that by the conventional method of moments (MOM), as well as the computing time and memory requirements. In addition, the influence of some parameters on the scattering of sea surface are investigated and discussed in detail, such as the threshold of coupling distance, iteration numbers, and windspeed.

1. INTRODUCTION

Electromagnetic scattering from randomly rough surface has been an popular topic of research, with applications in the fields of remote sensing, oceanography, communications, material science, electromagnetics and applied optics, etc. As a whole, methods in studying the rough surface scattering can be categorized into two groups, including analytical methods and numerical methods. The analytical methods are based on approximation techniques, among which the small perturbation method (SPM) [1], the Kirchhoff approximation (KA) [2, 3], and the small-slope approximation (SSA) [4] are of the most widely used. However, although these methods have the highest computational efficiency, they are restricted in domain of validity. For example, the KA [3], which is also referred to as the physical optics (PO) method, requires that every point on the rough surface have a large radius of curvature relative to the incident wavelength. In the other hand some numerical approaches, such as the method of moments (MOM) [5], the finite difference time-domain (FDTD) method [6], the finite element method (FEM) [7], and some fast algorithms based on them are also applied to the problem of EM scattering from rough surface. These numerical methods are capable of simulating surfaces with arbitrary roughness. But their computational cost is very high. Many practical problems such as the near-grazing incidence or rough sea surface with a large windspeeed are considered as large-scale rough surface problems. For such large-scale rough surface problems, a much larger surface length is required, and a more efficient method is needed. In this paper, the iterative physical optics (IPO) method is adopted to solve the scattering from randomly rough sea surface with large windspeed. At first, the IPO method is proposed and used to study the scattering by cavity [8, 9]. The IPO method is an improvement over the previous PO method. In PO method, the fields at any point on the surface are approximated by the local fields that would be present on the tangent plane at that point, which are irrelevant to the other points. But in IPO method, the multiple coupling interactions among points on rough surface are considered. This

Received 25 May 2017, Accepted 10 July 2017, Scheduled 4 August 2017
* Corresponding author: Juan Li (lijuan029@yeah.net).
The authors are with the School of Physics and Optoelectronic Engineering, Xidian University, No. 2, Taibai Road, Xi'an, Shaanxi, China.

will greatly improve the calculation accuracy. In addition, in the paper the local coupling technique is adopted to improve calculation efficiency.

The paper is organized as follows. In Section 2, the methodology of calculating scattering from 1-D PEC sea surface by IPO method is described, including the solution of induced current, solution of NRCS in the far zone, and local coupling technique, etc. Numerical validation and simulations are presented in Section 3. Section 4 ends with the conclusions of this paper and recommendations for further investigation of this topic. It should be noted that a time dependence of $e^{-\mathrm{i}\omega t}$ is assumed and suppressed throughout the paper.

2. SCATTERING FROM 1-D SEA SURFACE BY IPO METHOD

Figure 1 shows the geometry model of EM scattering from 1-D rough sea surface. To avoid artificial edge diffraction from the finite length rough surface, a Thorsos' tapered plane wave [5] is chosen and expressed as

$$\phi^{\mathrm{inc}}(\mathbf{r}) = \exp\left[i(\mathbf{k}_i \cdot \mathbf{r})(1 + w(\mathbf{r}))\right] \exp\left[-\frac{(x + z\tan\theta_i)^2}{g^2}\right] \tag{1}$$

where $w(\rho) = [2(x + z\tan\theta_i)^2/g^2 - 1]/(kg\cos\theta_i)^2$, g is the tapered factor, $\mathbf{r} = x\hat{\mathbf{x}} + z\hat{\mathbf{z}}$ the position vector, $\mathbf{k}_i = k(\sin\theta_i\hat{\mathbf{x}} - \cos\theta_i\hat{\mathbf{z}})$ the incident wave vector, and $\mathbf{k}_s = k(\cos\theta_s\hat{\mathbf{x}} + \sin\theta_s\hat{\mathbf{z}})$ the scattered wave vector. In the paper, one-dimensional (1-D) randomly rough sea surface profile with Pierson-Moskowitz (PM) spectrum is adopted and the power spectral density function [10] is defined as follows

$$W(K) = \frac{\alpha}{4\left|K\right|^3} \exp(-\frac{\beta g_c^2}{K^2U^4}) \tag{2}$$

Here K is the spatial wave number; $\alpha = 8.1 \times 10^{-3}$ and $\beta = 0.74$ are empirical constants; $g_c = 9.81\,\mathrm{m/s^2}$ is the gravitational acceleration constant; U is the wind speed at a height of 19.5 m. And the profile $\zeta(x)$ of sea surface is simulated by Monte Carlo method. For the sea surface with PM spectrum, the root-mean-square (rms) height δ are expressed as

$$\delta = \sqrt{\langle(\zeta(x))^2\rangle} = \sqrt{\int_{-\infty}^{+\infty} W(K)dK} = \sqrt{\frac{\alpha U^4}{4\beta g_c^2}} \tag{3}$$

In [10], the selection of the tapered factor g and finite surface length L have been fully investigated. Calculation finally yields

$$g > \frac{6\lambda}{(\cos\theta_i)^{1.5}} \quad L > 4g \tag{4}$$

$$L > 15l_c = 15\frac{5}{4g_c}\sqrt{\frac{3}{\beta}}U^2 \approx 3.8U^2\,(\mathrm{m}) \tag{5}$$

where, $l_c = 5/4g_c\sqrt{3U^2/\beta}$ is the correlation length of sea surface. From Eq. (4) and Eq. (5), it can be seen that the selections of g and L are related to the incident angle and wind speed. This denotes that the unknowns will dramatically increase with the increase of wind speed, especially for the high incident frequency.

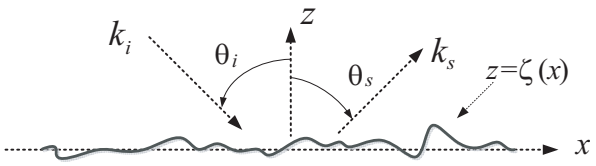

Figure 1. Geometry model from 1-D rough sea surface.

2.1. Solution of Induced Current in IPO Method

For HH polarization, the incident electric field is written as $\mathbf{E}^{inc}(\mathbf{r}) = \hat{\mathbf{y}}\phi^{inc}(\mathbf{r})$. Accordingly the incident magnetic field can be expressed as $\mathbf{H}^{inc}(\mathbf{r}) = \nabla \times \mathbf{E}^{inc}(\mathbf{r})/\mathrm{i}\omega\mu$ where ∇ is the Hamilton operator and μ is the permeability in free space. By PO theory [3], the surface current $\mathbf{J}^{(0)}(\mathbf{r}_i)$ at point $\mathbf{r}_i$ induced by incident tapered wave can be written as

$$\mathbf{J}^{(0)}(\mathbf{r}_i) = \begin{cases} 0 & \text{shadow} \\ 2\hat{\mathbf{n}}_i \times \mathbf{H}^{\mathrm{inc}}(\mathbf{r}_i) = -2\hat{\mathbf{y}}[\hat{\mathbf{n}}_i \cdot \nabla\phi^{\mathrm{inc}}(\mathbf{r}_i)]/\mathrm{i}\omega\mu & \text{lit} \end{cases} \tag{6}$$

where $\hat{\mathbf{n}}_i$ denotes the unit normal vector at point $\mathbf{r}_i$ on sea surface. For convenience, Eq. (6) is rewritten as

$$\begin{cases} \mathbf{J}^{(0)}(\mathbf{r}_i) = \dfrac{-2\hat{\mathbf{y}}}{\mathrm{i}\omega\mu} J_0(\mathbf{r}_i) \\ J^{(0)}(\mathbf{r}_i) = \begin{cases} 0 & \text{shadow} \\ \hat{\mathbf{n}}_i \cdot \nabla\phi^{\mathrm{inc}}(\mathbf{r}_i) & \text{lit} \end{cases} \end{cases} \tag{7}$$

With the increase of windspeed, sea surface will become rougher. In this case, the multiple coupling interactions among points on sea surface need to be considered to obtain more accurate result. Taken any point on sea surface $\mathbf{r}_i$ for example, at point $\mathbf{r}_i$ the scattered field $\mathbf{E}^{(1)}(\mathbf{r}_i)$ excited by $\mathbf{J}^{(0)}(\mathbf{r}_j)\,(j = 1 \sim N, j \neq i)$ at the other point on sea surface is

$$\mathbf{E}^{(1)}(\mathbf{r}_i) = \mathrm{i}\omega\mu \sum_{j\neq i}^{N} \left(\bar{\bar{I}} + \frac{\nabla\nabla}{k^2}\right) G(\mathbf{r}_i, \mathbf{r}_j) \cdot \mathbf{J}^{(0)}(\mathbf{r}_j) ds \tag{8}$$

where N represents the number of the discrete points on sea surface, $\bar{\bar{I}}$ the unit tensor, $G(\mathbf{r}_i, \mathbf{r}_j) = \mathrm{i}\mathrm{H}_0^{(1)}(\mathrm{k}|\mathbf{r}_\mathrm{i} - \mathbf{r}_\mathrm{j}|)/4$ the scalar Green's function in 2-D space, and $H_0^{(1)}(k|\mathbf{r}_i - \mathbf{r}_j|)$ the zero-order Hankel function of the first kind. Substituting Eq. (7) into Eq. (8), $\mathbf{E}^{(1)}(\mathbf{r}_i)$ can be rewritten as

$$\begin{aligned} \mathbf{E}^{(1)}(\mathbf{r}_i) &= \mathrm{i}\omega\mu \sum_{j\neq i}^{N} \left(\bar{\bar{I}} + \frac{\nabla\nabla}{k^2}\right) G(\mathbf{r}_i, \mathbf{r}_j) \cdot \left[\frac{-2\hat{\mathbf{y}}}{\mathrm{i}\omega\mu} J^{(0)}(\mathbf{r}_j)\right] ds \\ &= -\hat{\mathbf{y}}\frac{\mathrm{i}}{2} \sum_{j\neq i}^{N} J^{(0)}(\mathbf{r}_j) H_0^{(1)}(k\,|\mathbf{r}_i - \mathbf{r}_j|) ds \end{aligned} \tag{9}$$

And the corresponding magnetic field is equal to $\mathbf{H}^{(1)}(\mathbf{r}_i) = \nabla \times \mathbf{E}^{(1)}(\mathbf{r}_i)/\mathrm{i}\omega\mu$. Thus the 1st-order coupled current $\mathbf{J}^{(1)}(\mathbf{r}_i)$ at point $\mathbf{r}_i$ in the lit area can be acquired by PO method

$$\begin{aligned} \mathbf{J}^{(1)}(\mathbf{r}_i) &= 2\hat{\mathbf{n}}_i \times \mathbf{H}^{(1)}(\mathbf{r}_i) \\ &= -\frac{1}{\omega\mu}\hat{\mathbf{n}}_i \times \sum_{i\neq j}^{N} J^{(0)}(\mathbf{r}_j) \nabla \times \left[\hat{\mathbf{y}} H_0^{(1)}(k\,|\mathbf{r}_i - \mathbf{r}_j|)\right] ds \\ &= -\hat{\mathbf{y}}\frac{k}{\omega\mu} \sum_{i\neq j}^{N} J^{(0)}(\mathbf{r}_j) \left(\hat{\mathbf{n}}_i \cdot \hat{\mathbf{R}}_{ij}\right) H_1^{(1)}(k\,|\mathbf{r}_i - \mathbf{r}_j|) ds \end{aligned} \tag{10}$$

where $\hat{\mathbf{R}}_{ij} = \mathbf{r}_i - \mathbf{r}_j/|\mathbf{r}_i - \mathbf{r}_j|$ denotes a unit vector, and $H_1^{(1)}(k|\mathbf{r}_i - \mathbf{r}_j|)$ represents the first-order Hankel function of the first kind. Similar to Eq. (7), Eq. (10) yields

$$\begin{cases} \mathbf{J}^{(1)}(\mathbf{r}_i) = -\hat{\mathbf{y}}\frac{k}{\omega\mu} J^{(1)}(\mathbf{r}_i) \\ J^{(1)}(\mathbf{r}_i) = \begin{cases} 0 & \text{shadow} \\ \displaystyle\sum_{i\neq j}^{N} J^{(0)}(\mathbf{r}_j) \left(\hat{\mathbf{n}}_i \cdot \hat{\mathbf{R}}_{ij}\right) H_1^{(1)}(k\,|\mathbf{r}_i - \mathbf{r}_j|) ds & \text{lit} \end{cases} \end{cases} \tag{11}$$

In the same way, the 2nd-order coupled current $\mathbf{J}^{(2)}(\mathbf{r}_i)$ is written as

$$\begin{cases} \mathbf{J}^{(2)}(\mathbf{r}_i) = \hat{\mathbf{y}}\dfrac{k^2}{2\mathrm{i}\omega\mu}J^{(2)}(\mathbf{r}_i) \\ J^{(2)}(\mathbf{r}_i) = \begin{cases} 0 & \text{shadow} \\ \displaystyle\sum_{i\neq j}^{N} J^{(1)}(\mathbf{r}_j)\left(\hat{\mathbf{n}}_i\cdot\hat{\mathbf{R}}_{ij}\right)H_1^{(1)}(k\left|\mathbf{r}_i-\mathbf{r}_j\right|)ds & \text{lit} \end{cases} \end{cases} \tag{12}$$

By analogy, we can obtain the conclusion that the nth-order coupled current $\mathbf{J}^{(n)}(\mathbf{r}_i)$ is related to the $n-1$th-order coupled current $\mathbf{J}^{(n-1)}(\mathbf{r}_i)$. When $n \geq 2$, the relations between them are as follows

$$\begin{cases} \mathbf{J}^{(n)}(\mathbf{r}_i) = \dfrac{-2\hat{\mathbf{y}}}{\mathrm{i}\omega\mu}\left(\dfrac{\mathrm{ik}}{2}\right)^{n-1}J^{(n)}(\mathbf{r}_i) \\ J^{(n)}(\mathbf{r}_i) = \begin{cases} 0 & \text{shadow} \\ \displaystyle\sum_{i\neq j}^{N} J^{(n-1)}(\mathbf{r}_j)\left(\hat{\mathbf{n}}_i\cdot\hat{\mathbf{R}}_{ij}\right)H_1^{(1)}(k\left|\mathbf{r}_i-\mathbf{r}_j\right|)ds & \text{lit} \end{cases} \end{cases} \tag{13}$$

Thus, the total surface current on sea surface for multiple coupled scattering can be written as

$$\begin{aligned} \mathbf{J}^{total}(\mathbf{r}_i) &= \frac{-2\hat{\mathbf{y}}}{\mathrm{i}\omega\mu}\left[J^{(0)}(\mathbf{r}_i)+\left(\frac{\mathrm{ik}}{2}\right)J^{(1)}(\mathbf{r}_i)\ldots+\left(\frac{\mathrm{ik}}{2}\right)^{n-1}J^{(n)}(\mathbf{r}_i)\ldots\right] \\ &= \frac{-2\hat{\mathbf{y}}}{\mathrm{i}\omega\mu}J^{total}(\mathbf{r}_i) \end{aligned} \tag{14}$$

And for VV polarization, the incident magnetic field is written as $\mathbf{H}^{\mathrm{inc}}(\mathbf{r}) = \hat{\mathbf{y}}\phi^{\mathrm{inc}}(\mathbf{r})$. By the IPO method, the coupled surface currents $\mathbf{J}^{(n)}(\mathbf{r}_i)\,(n=1,2,3,4\ldots)$ can be derived similarly, which are not presented due to the limitation of length.

2.2. Solution of NRCS in the Far Zone

For HH polarization, in the far-field region the scattered field $\mathbf{E}^{sct}(\mathbf{r}_\infty)$ excited by the total surface current $\mathbf{J}^{total}(\mathbf{r}_i)$ can be obtained by equivalent principle

$$\begin{aligned} \mathbf{E}^{sct}(\mathbf{r}_\infty) &= \mathrm{i}\omega\mu\int\left(\bar{\bar{I}}+\frac{\nabla\nabla}{k^2}\right)G(\mathbf{r}_\infty,\mathbf{r}_i)\cdot\mathbf{J}^{total}(\mathbf{r}_i)ds \\ &= \frac{\hat{\mathbf{y}}}{2\mathrm{i}}\int H_0^{(1)}(k\left|\mathbf{r}_\infty-\mathbf{r}_i\right|)J^{total}(\mathbf{r}_i)ds \\ &\approx \frac{\hat{\mathbf{y}}}{2\mathrm{i}}\sqrt{\frac{2}{\pi kr_\infty}}e^{\mathrm{ikr}_\infty}e^{-\mathrm{i}\frac{\pi}{4}}\int J^{total}(\mathbf{r}_i)e^{-\mathrm{i}\mathbf{r}_\infty\cdot\mathbf{k}_s}ds \\ &= \frac{\hat{\mathbf{y}}}{2\mathrm{i}}\sqrt{\frac{2}{\pi kr_\infty}}e^{\mathrm{ikr}_\infty}e^{-\mathrm{i}\frac{\pi}{4}}E^{sct}(\mathbf{r}_\infty) \end{aligned} \tag{15}$$

For convenience, let $E^{sct}(\mathbf{r}_\infty) = \int J^{total}(\mathbf{r}_i)e^{-\mathrm{i}\mathbf{r}_\infty\cdot\mathbf{k}_s}ds$. $\mathbf{r}_\infty$ represents the observation point in far zone and is a function of scattered angle θ_s. Therefore, $\mathbf{E}^{sct}(\mathbf{r}_\infty)$ and $E^{sct}(\mathbf{r}_\infty)$ can also be denoted as $\mathbf{E}^{sct}(\theta_s)$ and $E^{sct}(\theta_s)$, respectively.

Thus, the normalized radar cross section (NRCS) in the far-field zone is defined as that in [11]

$$\sigma(\theta_s) = \frac{\left|E^{sct}(\theta_s)\right|^2}{2\pi kg\sqrt{\pi/2}\cos\theta_i\left[1-\dfrac{1+2\tan^2\theta_i}{2(kg\cos\theta_i)^2}\right]} \tag{16}$$

And the NRCS in the far zone for VV polarization can be derived similarly, which is not given here.

2.3. Local Coupling Technique

In iterative PO, all interactions between nearby points and non-nearby points are considered. Thus, it is difficult to efficiently deal with the scattering from a large-scale sea surface because of the expensive interaction time. But in fact, only the coupling interactions between local points are dominant. That's to say, the coupling interaction between points $\mathbf{r}_i$ and $\mathbf{r}_j$ on sea surface decreases with the increase of the distance $|\mathbf{r}_i - \mathbf{r}_j|$. When the distance reaches a threshold, it can be seen approximately as the non-coupling interaction between the two points. Therefore, in the iterative process, the coupling interactions between far-zone points can be neglected within a certain accuracy range. The method is called as the local coupling technique and is firstly mentioned in reference [12], which can greatly reduce the computational cost. And the distance threshold l will be analyzed in the following numerical results.

3. NUMERICAL RESULTS

In the following numerical simulations, by IPO method the EM scattering from 1-D randomly rough sea surface with large windspeed is solved and analyzed in detail. Unless noted otherwise, a sea surface is generated with a discretization rate of 10 points per wavelength. And the numerical results are averaged by 50 Monte Carlo realizations throughout the paper. In addition, all simulations are obtained on a computer with a 2.0 GHz processor (Intel Core 2 Duo E2180 CPU), 2GB memory, and Visual Fortran 6.5 compiler.

To ensure the validity of our method, in Fig. 2 the NRCS of 1-D PEC rough sea surface is solved by the PO method, IPO method, and conventional MOM method [7], respectively. Both HH and VV polarizations are concluded. Where the incident tapered wave is given by $f = 0.3\,\text{GHz}(\lambda = 1.0\,\text{m})$ and $\theta_i = 40°$. And the windspeed U is equal to 10 m/s. To satisfy Eq. (4) and Eq. (5), the length of rough surface is set as $L = 409.6\lambda$. And the distance threshold $l = 30\lambda$ is adopted. In Fig. 2 it is readily observed that the NRCS by PO method is in good agreement with the result by MOM method only in the small and moderate scattering angle regions. But the result by IPO method can match very well with that of the MOM method for most observation angles, especially for VV polarization. This demonstrates a good accuracy of our present method. In addition, the comparisons of computer resource consumed in memory and time for one realization by IPO and MOM are also demonstrated in Table 1. The memory by our method is only 0.62% of that by MOM. And the calculation times consumed by IPO are about 24.4% and 11.23% of those by MOM for VV and HH polarizations, respectively.

The validity of the presented approach in solving EM scattering from rough sea surface with larger

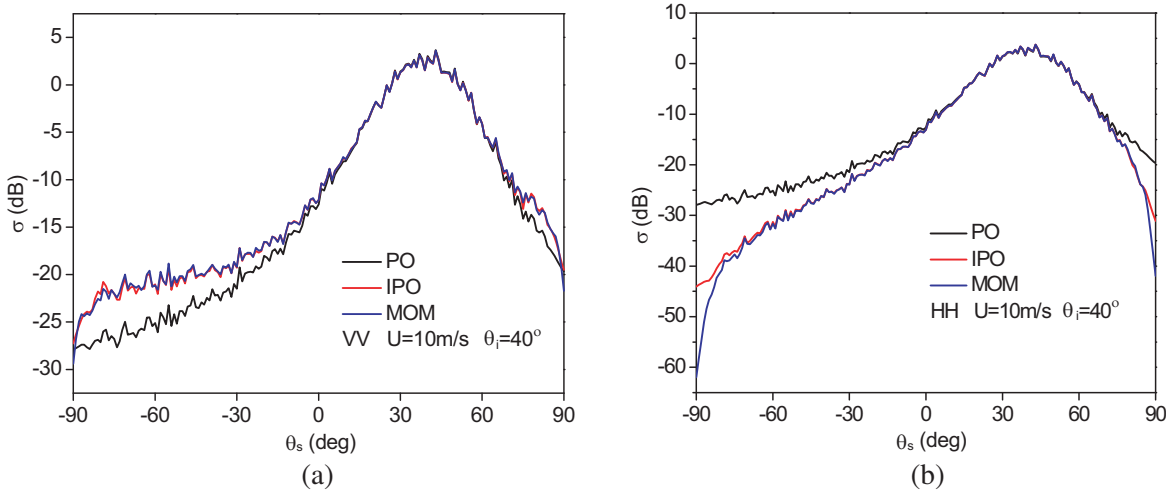

Figure 2. Comparison of NRCS from sea surface solved by PO, IPO, MOM. $U = 10\,\text{m/s}$. (a) VV, (b) HH.

Table 1. Comparison of computer resource for one realization ($U = 10\,\mathrm{m/s}$).

Polarization	Method	Memory (MB)	Time (s)
VV	MOM	257.8	41
	IPO	1.59	10
HH	MOM	257.8	89
	IPO	1.59	10

wind speed ($U = 14\,\mathrm{m/s}$) is shown in Fig. 3. Scattering behaviors are observed with incident angle $\theta_i = 60°$ and frequency $f = 0.3\,\mathrm{GHz}$. The length of sea surface is set as $L = 819.2\lambda$. Also, it can be seen that the angular distribution of NRCS obtained by IPO method matches very well with that by MOM method for most observed angles. Moreover, Table 2 depicts the memory and computational time needed by the two methods for one realization. The memory is reduced to 0.22% of that in the conventional MOM. And the computational time using IPO are 8.27% and 3.51% of those using MOM for VV and HH polarizations, respectively. This indicates that the proposed method requires less memory and time, especially for the EM scattering from a large-scale rough sea surface.

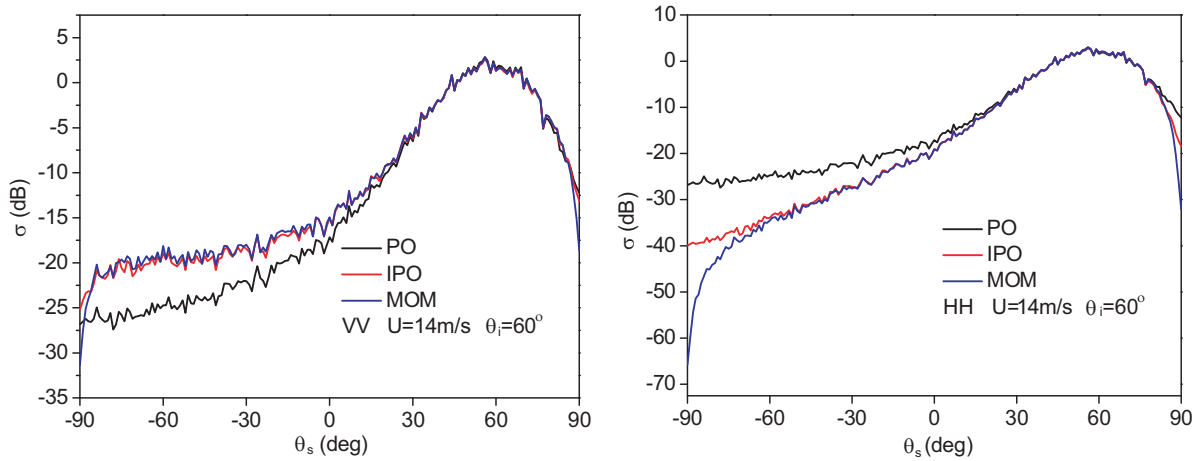

Figure 3. Comparison of scattering from sea surface solved by PO, IPO, MOM. $U = 14\,\mathrm{m/s}$. (a) VV, (b) HH.

Table 2. Comparison of computer resource for one realization ($U = 14\,\mathrm{m/s}$).

Polarization	Method	Memory (MB)	Time (s)
VV	MOM	1027.71	254
	IPO	2.29	21
HH	MOM	1027.71	598
	IPO	2.29	21

To explain the selection of the distance threshold in local coupling technique, in Fig. 4 at a specific point the currents induced by the rest of points on sea surface are presented in the 1st-order coupling scattering. Where any three points are selected to be analyzed, including the central point of sea surface, two points which are 60λ away from central point on the left and on the right, respectively. The parameters of the incident wave and sea surface are the same as those described in Fig. 2, and a

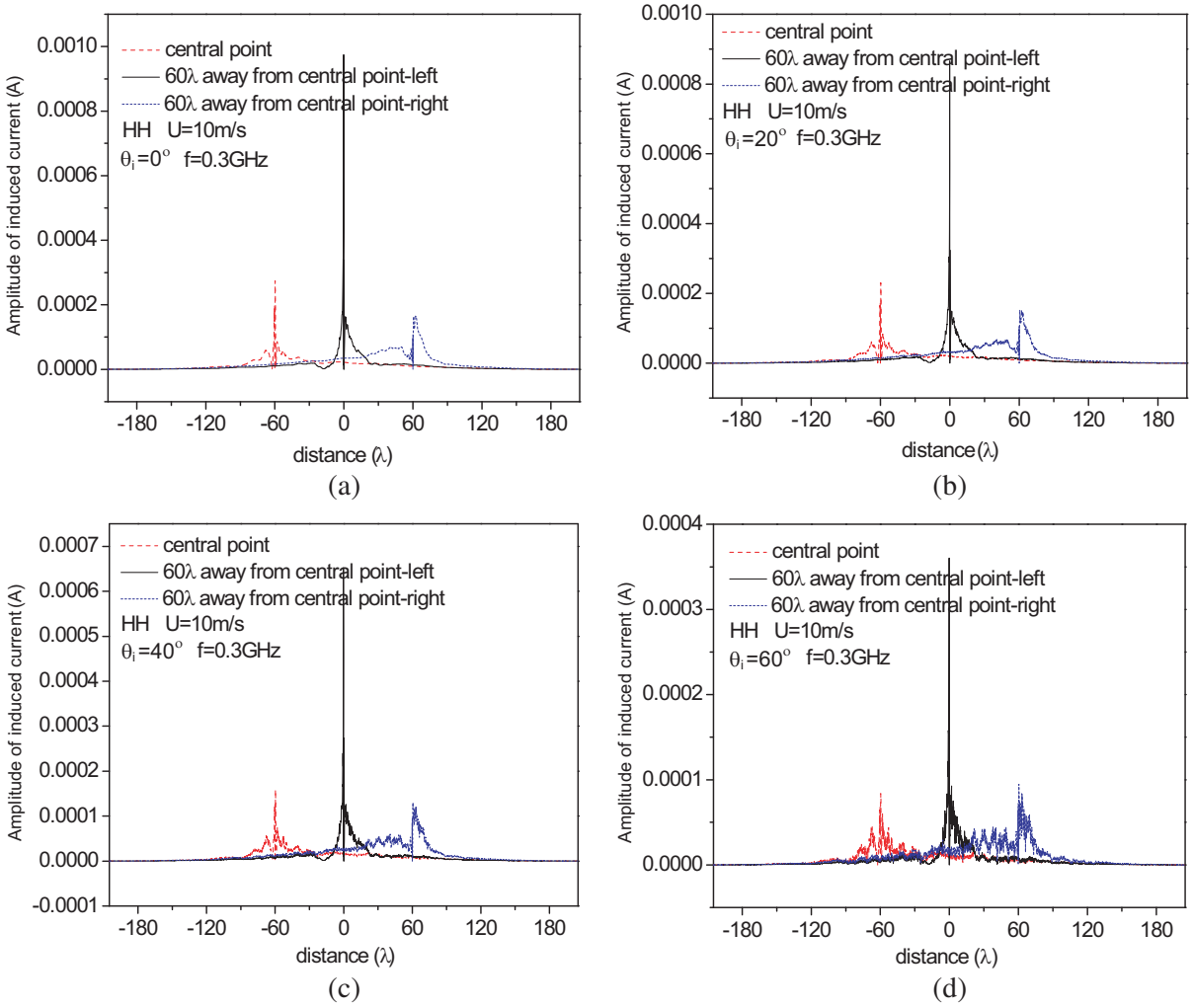

Figure 4. Distribution of current at a specific point induced by the rest of points on sea surface in the 1st-order coupling scattering. (a) $\theta_i = 0°$, (b) $\theta_i = 20°$, (c) $\theta_i = 40°$, (d) $\theta_i = 60°$.

tapered wave with HH polarization for one realization is considered. We can observe that the amplitude of induced current near specific point has a relatively big value, and it is almost attenuated to zero at the location which is about $20\lambda \sim 60\lambda$ away from specific point. This illustrates that the induced currents in local region are dominant, and when the distance of any two points on sea surface reaches to a certain value, the coupling interaction between them can be neglected. In addition, a conclusion is obtained that the threshold of distance is about $20\lambda \sim 60\lambda$ by our enormous experiments for different incident angle, frequency, windspeed, etc.

For the rough sea surface ($L = 1638.4\lambda$, $U = 10\,\mathrm{m/s}$), in Fig. 5 the distributions of induced current with HH polarization are compared for different numbers of couplings, as well as the NRCS of sea surface by IPO method with increase of the number of couplings. The parameters of the tapered wave are presented by $f = 1.0\,\mathrm{GHz}$ ($\lambda = 0.3\,\mathrm{m}$) and $\theta_i = 50°$. Fig. 5(a) shows the induced surface currents along the rough sea surface for the 0th-order (i.e., direct scattering), 1st-order, 3rd-order, and 5th-order coupling scattering, respectively. It is obvious that the amplitude of coupled current is much less than that of the 0th-order induced surface current. This indicates that the contribution of direct scattered field is dominant in the total scattered fields. Moreover, we also observe that with increasing of the number of couplings, the amplitude of induced current becomes smaller and smaller. Fig. 5(b) illustrates the NRCS of sea surface solved by IPO method when the 1st-order, 3rd-order, and 5th-order coupling scatterings are concluded, respectively. In addition, due to the enormous unknowns, the

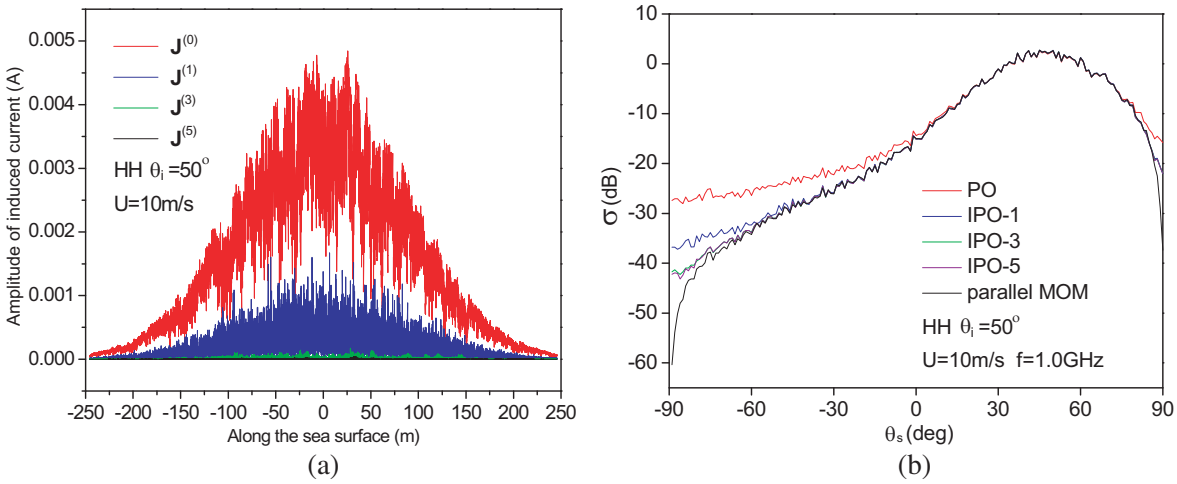

Figure 5. Comparisons of induced surface current and NRCS for different number of couplings. (a) Induced current. (b) NRCS.

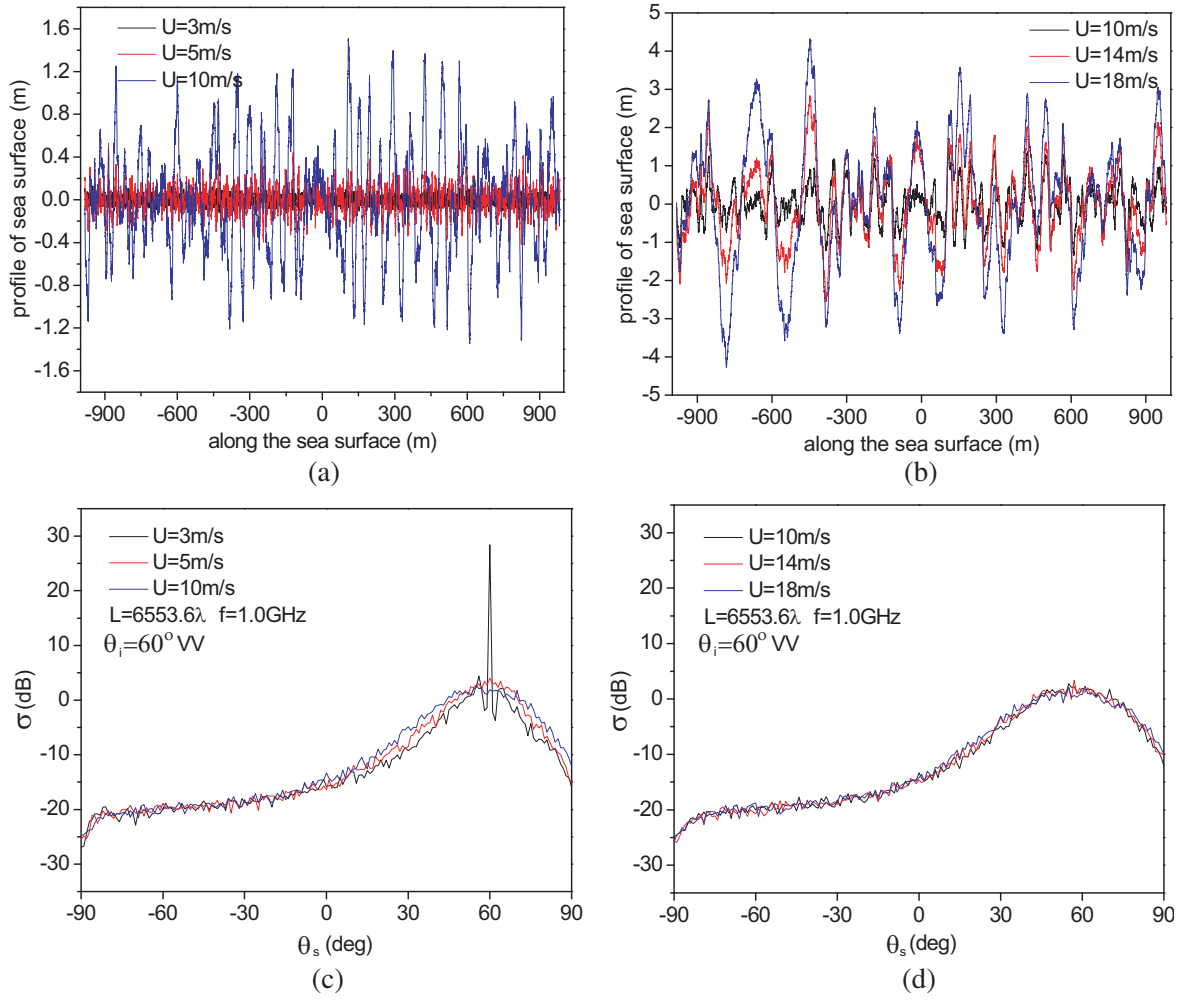

Figure 6. Profile and scattering from sea surface with different windspeeds. (a) Profile ($3 \sim 10$ m/s), (b) profile ($10 \sim 18$ m/s), (c) NRCS ($3 \sim 10$ m/s), (d) NRCS ($10 \sim 18$ m/s).

memory requirement of the conventional MOM method becomes too large for the PC used to conduct the calculation. Therefore, the parallel MOM method based on MPI library [13] is adopted in Fig. 5(b). It is found that when the 1st-order coupling scattering is considered, the result by IPO method (i.e., IPO-1) has an obvious improvement over that of PO method. And the curve by using IPO-3 method has also a little improvement over that of IPO-1 method. But the result by IPO-5 method is nearly identical to that of IPO-3 method. This illustrates that when the number of couplings reaches a certain value, the scattering results by sea surface will keep stable.

To further explore the important scattering characteristics of sea surface, the profile and scattering from sea surface with VV polarization are investigated for different windspeeds ($3 \sim 18\,\mathrm{m/s}$), where the incident frequency is $f = 1.0\,\mathrm{GHz}$ ($\lambda = 0.3\,\mathrm{m}$), and incident angle is $\theta_i = 60°$. In this case, the length of sea surface should be larger than 1231.2 m at least according to Eq. (4) and Eq. (5). So here the length $L = 6553.6\lambda$ is selected. In Figs. 6(a) and (b), the profiles of sea surface are presented. It is obvious that with the increase of windpeed, the height of sea surface with PM spectrum increases dramatically. And in Fig. 6(c) the curves of NRCS are shown with windspeed 3 m/s, 5 m/s, and 10 m/s, respectively. We can observe that in the specular direction the NRCS becomes smaller with increasing of windspeed, especially with windspeed 3 m/s there is a significant peak. And near the specular direction, the NRCS becomes larger gently with the increase of windspeed. But in the other directions, the change of NRCS with windspeed is not obvious. In addition, Fig. 6(d) denotes the scattering results with larger windspeeds (10 m/s, 14 m/s, and 18 m/s). Likewise, it is difficult to distinguish the curves over the whole scattered angles. From Fig. 6(c) and Fig. 6(d), as a whole, the change of scattering from sea surface with windspeed is not obvious, which is different from the profile of sea surface.

4. CONCLUSIONS

In the paper, the efficient iterative PO method is applied to calculate EM scattering from a PEC rough sea surface for both HH and VV polarizations. The formulae of calculating induced surface currents on rough sea surface for multiple scattering are derived in detail. The validity of the proposed method is shown by comparing it with the conventional MOM method. Numerical results show that the present method can work very well and requires less memory and computational time. Our future study could deal with the EM scattering of a 1-D dielectric rough surface by the IPO method, as well as the EM scattering from a 2-D rough surface.

ACKNOWLEDGMENT

This work was supported by the National Natural Science Foundation for Distinguished Young Scholars of China (Grant No. 61225002), the National Natural Science Foundation of China (Grant No. 61501360). The authors thank the reviewers for their helpful and constructive suggestions.

REFERENCES

1. Dusséaux, R., S. Afifi, and R. D. Oliveira, "On the stationarity of signal scattering by two-dimensional slightly rough random surfaces," *IEEE Trans. Antennas Propag.*, Vol. 61, No. 11, 5828–5832, 2013.
2. Iodice, A., A. Natale, and D. Riccio, "Kirchhoff scattering from fractal and classical rough surfaces: Physical interpretation," *IEEE Trans. Antennas Propag.*, Vol. 61, No. 4, 2156–2163, 2013.
3. Tabatabaeenejad, A., X. Y. Duan, and M. Moghaddam, "Coherent scattering of electromagnetic waves from two-layer rough surfaces within the Kirchhoff regime," *IEEE Trans. Geosci. Remote Sensing*, Vol. 51, No. 7, 3943–3953, 2013.
4. Wei, P. B., M. Zhang, R. Q. Sun, and X. F. Yuan, "Scattering studies for two-dimensional exponential correlation textured rough surfaces using small-slope approximation method," *IEEE Trans. Geosci. Remote Sensing*, Vol. 52, No. 9, 5364–5373, 2014.
5. Ding, K. H., L. Tsang, and J. A. Kong, *Scattering of Electromagnetic Wave: Numerical Simulations*, Wiley-Inter-science, New York, NY, USA, 2001.

6. Li, J., L. X. Guo, H. Zeng, and X. B. Han, "Message-passing-interface-based parallel FDTD investigation on the EM scattering from a 1-D rough sea surface using uniaxial perfectly matched layer absorbing boundary," *J. Opt. Soc. Am. A*, Vol. 26, No. 6, 1494–1502, 2009.
7. Khankhoje, U. K., J. J. Vanzyl, and T. A. Cwik, "Computation of radar scattering from heterogeneous rough soil using the finite-element method," *IEEE Trans. Geosci. Remote Sensing*, Vol. 51, No. 6, 3461–3469, 2013.
8. Basteiro, F. O., J. L. Rodriguez, and R. J. Burkholder, "An iterative physical optics approach for analyzing the electromagnetic scattering by large open-ended cavities," *IEEE Trans. Antennas Propag.*, Vol. 43, No. 4, 356–361, 1995.
9. Burkholder, R. J. and T. Lundin, "Forward-backward iterative physical optics algorithm for computing the RCS of open-ended cavities," *IEEE Trans. Antennas Propag.*, Vol. 53, No. 2, 793–799, 2005.
10. Ye, H. X. and Y. Q. Jin, "Parameterization of the tapered incident wave for numerical simulation of electromagnetic scattering from rough surface," *IEEE Trans. Antennas Propag.*, Vol. 53, No. 3, 1234–1237, 2005.
11. Thorsos, E. I., "The validity of the Kirchhoff approximation for rough surface scattering using a Gaussian roughness spectrum," *J. Acoust. Soc. Amer.*, Vol. 83, No. 1, 78–92, 1988.
12. Hu, J., Z. P. Nie, L. Lei, and Y. P. Chen, "Solving 3D electromagnetic scattering and radiation by local multilevel fast multipole algorithm," *IEEE International Symposium on Microwave, Antenna, Propagation and EMC Technologies for Wireless Communications Proceedings*, 619–622, 2005.
13. Guo, L. X., A. Q. Wang, and J. Ma, "Study on EM scattering from 2-D target above 1-D large scale rough surface with low grazing incidence by parallel MOM based on PC clusters," *Progress In Electromagnetics Research*, Vol. 89, 149–166, 2009.